Journal of Materials Chemistry

Cite this: *J. Mater. Chem.*, 2012, **22**, 16833

www.rsc.org/materials

PAPER

A novel fabrication of a well distributed and aligned carbon nanotube film electrode for dye-sensitized solar cells†

Sanqing Huang,‡ Zhibin Yang,‡ Lingli Zhang, Ruixuan He, Tao Chen, Zhenbo Cai, Yongfeng Luo, Huijuan Lin, Hui Cao, Xingrong Zhu and Huisheng Peng*

Received 29th March 2012, Accepted 26th June 2012
DOI: 10.1039/c2jm31954c

Carbon nanotubes (CNTs) have been recently fabricated into macroscopic films to improve their practical applications in a wide variety of fields, *e.g.* electrode materials. In the current CNT electrodes however, CNTs are typically interconnected to form networks or are aligned as lots of bundles, and the resulting photovoltaic devices based on the CNT electrodes have typically shown low energy conversion efficiencies. Here we report a new and general drying approach to make a well distributed and aligned CNT film which exhibits a rapid charge separation and transport. As a demonstration, it has been used as a counter electrode to fabricate dye-sensitized solar cells with an energy conversion efficiency of 9.05%.

Introduction

Photovoltaics may represent a general and efficient approach to solve the global energy crisis, and have attracted extensive attention from both academia and industry for many years.[1–3] However, the development of inorganic photovoltaics has long been hindered by complex fabrication and high costs. As a result, increasing interest has been recently paid to dye-sensitized solar cells which can be fabricated by an easy solution process with low cost.[4–6] In this case, it is critically important to further increase the cell efficiency. The conventional electrode materials based on noble metals, such as platinum, have obvious limitations, *e.g.* being expensive with limited supply on the earth, being prepared by deposition under vacuum and being unstable during use.[7,8] Therefore, a lot of effort has been used to discover new electrode materials in replacement of platinum.

Carbon nanotubes (CNTs) represent one of the most promising candidates due to their combined advantages which include high surface area, high stability, and excellent electrical and electrocatalytic properties.[9,10] The CNT electrodes typically in the format of film have been mainly prepared by coating CNT dispersions onto substrates.[11,12] As CNTs randomly aggregate into network structures during the evaporation of solvents, it remains challenging to control the film structure, and the generated charges also have to transport among a large number of crossed contacting points with low efficiency when randomly dispersed CNT films are used as electrodes. To this end, aligned CNT sheets have been recently drawn from spinnable CNT arrays and were expected to show promising applications for efficient electrode materials.[13,14]

However, we recently found that these sheets were composed of a lot of CNT bundles. Fig. 1 shows a typical scanning electron microscopy (SEM) image of a multi-walled carbon nanotube (MWCNT) sheet. The MWCNTs are not uniformly dispersed in the sheet. Therefore, it is difficult to control and improve the MWCNT structure. Both the stability and electrical conductivity also need to be improved. In addition, when the MWCNT sheet was used as the counter electrode to fabricate dye-sensitized solar cells, the resulting cells showed lower power conversion efficiencies than the conventional platinum. Herein, we have developed a new and general peeling approach to prepare well distributed and aligned MWCNT films. These films showed a much higher efficiency than both MWCNT sheets and platinum as the counter electrode in dye-sensitized solar cells.

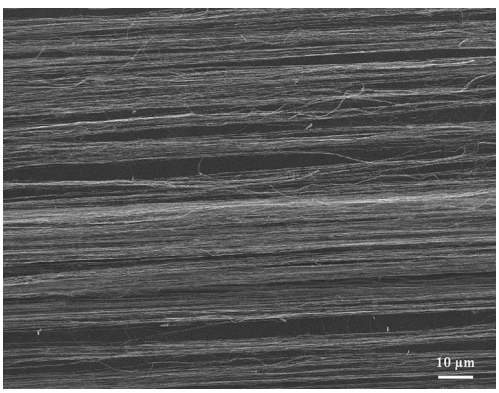

Fig. 1 Scanning electron microscopy (SEM) image of a MWCNT sheet.

State Key Laboratory of Molecular Engineering of Polymers, Department of Macromolecular Science, Laboratory of Advanced Materials, Fudan University, Shanghai 200438, China. E-mail: penghs@fudan.edu.cn

† Electronic supplementary information (ESI) available. See DOI: 10.1039/c2jm31954c

‡ These authors contributed equally to this work.

Experimental section

MWCNT arrays were grown by chemical vapor deposition with Fe (1 nm)/Al_2O_3 (10 nm) as the catalyst at 750 °C.[15] Ethylene was used as the carbon source and a mixture of Ar and H_2 was used as the carrying gas. The flow rate ratios of Ar, H_2, and C_2H_4 were 400, 25, and 75 sccm, respectively. The thickness of the MWCNT array could be up to 4 mm. The synthesized MWCNTs showed a diameter of ~10 nm. A tape was then used to touch the top edge of an array to paste the desired MWCNTs which could be transferred onto various substrates such as a glass slide, fluorine-doped tin oxide and polymers. The MWCNT number density was further increased after a solvent treatment by ethanol or/and pressing treatment. As a comparison, MWCNT sheets were obtained from spinnable MWCNT arrays with heights of 200–300 μm. In a typical spinning process, a MWCNT ribbon was first drawn from the CNT array and a microprobe was then used to touch the ribbon to continuously pull it out of the MWCNT sheet. The synthesis of the spinnable MWCNT arrays was previously reported elsewhere.[16–18]

For application as the counter electrode in dye-sensitized solar cells, the MWCNT films were transferred onto fluorine-doped tin oxide glass (15 ohm per square) or flexible indium tin oxide on polyethylene naphthalate (15 ohm per square), followed by heating at 500 °C in argon for the first case and 150 °C in air for the second case. In the case of platinum as the counter electrode, it was coated onto fluorine-doped tin oxide glass by thermal decomposition of H_2PtCl_6.[19] The working electrode was composed of a layer of nanocrystalline TiO_2 (diameter of 20 nm) with a thickness of 14 μm and a light-scattering layer of TiO_2 (diameter of 200 nm) with thickness of 2 μm prepared by screen printing technology. The area of TiO_2 electrodes was 0.25 cm^2. The working electrode was heated to 500 °C for 30 min and annealed in air. It was then immersed in aqueous 40 mM $TiCl_4$ at 60 °C for 25 min and washed with deionized water and ethanol, followed by sintering at 500 °C for 30 min. After the temperature was decreased to 120 °C, it was immersed into 0.3 mM N719 solution in dehydrated acetonitrile and *tert*-butanol (volume ratio of 1 : 1) for ~16 h. The N719-incorporated electrode was carefully rinsed by dehydrated acetonitrile. The working and counter electrodes with a Surlyn frame as the spacer were sealed by pressing them together at a pressure of about 0.2 MPa and a temperature of 125 °C. The redox electrolyte (composed of 0.1 M lithium iodide, 0.05 M iodine, 0.6 M 1,2-dimethyl-3-propylimidazolium iodide and 0.5 M 4-*tert* butyl-pyridine in dehydrated acetonitrile) was introduced into the cell through the back hole of the counter electrode. Finally, the hole was sealed with the Surlyn and a cover glass. In the case of a flexible cell, a TiO_2 mixture with 80% anatase and 20% rutile was added to ethanol with a concentration of 20 wt%. The suspension was coated onto the conducting substrate by a doctor blading method to produce the working electrode.

The film thickness was measured by a Dektak 150 Step Profiler. The structure was characterized by scanning electron microscopy (Hitachi FE-SEM S-4800 operated at 1 kV). Raman measurement was performed on a Renishaw inVia Reflex with excitation wavelength of 514.5 nm and laser power of 20 mW. The electrical conductivity was obtained by a physical property measurement system (KEITHLEY 2182A nanovoltmeter with 6221A DC and AC current source). The resistivity change under bending was monitored by Agilent 34401A digital multimeter. The dye-sensitized solar cells were measured by recording *J–V* curves with a Keithley 2400 Source Meter under illumination (100 mW cm^{-2}) of simulated AM 1.5 solar light coming from a solar simulator (Oriel-Sol3A 94023A equipped with a 450 W Xe lamp and an AM 1.5 filter). The stray light was shielded by a mask with an aperture which was a little smaller than the working electrode. Cyclic voltammetry and electrochemical impedance spectroscopy were performed on a CHI 660a electrochemical workstation.

Results and discussion

Fig. 2 shows schematically the preparation of the well distributed and aligned MWCNT film. MWCNT arrays were first grown by a chemical vapor deposition process with thicknesses of millimeters (Fig. S1†). Rows of MWCNTs were then peeled off from the top edge of a MWCNT array by a normal tape and transferred onto the desired substrate. The MWCNT number density of the cross section in the as-prepared film was typically ~1×10^{10} cm^{-2}. The MWCNT number density corresponds to the plane perpendicular to the MWCNT-aligned direction in this work, it can be further increased and tuned by solvent or/and pressing treatments. Fig. 3 shows scanning electron microscopy (SEM) images of the MWCNT films with increasing MWCNT number densities of ~1×10^{10} cm^{-2}, ~1×10^{11} cm^{-2}, ~3×10^{11} cm^{-2} and ~4×10^{11} cm^{-2}. The MWCNTs were well distributed and aligned before and after treatments. Fig. S2† shows a typical Raman spectrum of the resulting MWCNT materials with high quality.[13–15] The thickness of the aligned MWCNT film was controlled by varying the contact width of the tape or/and the above post-treatment. In this work, the MWCNT film has been mainly prepared with the thickness range of 200 nm to 20 μm. Due to the large surface area, the MWCNT film can be easily and stably attached onto a wide variety of substrates such as glass, fluorine-doped tin oxide and polymers through van der Waals forces. For instance, Fig. S3† shows that a flexible MWCNT film stabilized on poly (ethylene naphthalate) can be bent for more than one hundred cycles without obvious structure changes traced by SEM, *i.e.*, the MWCNTs remained highly aligned and attached on the polymer substrate.

Electrical conductivities of the MWCNT films were measured along both length and width directions by a two-probe method. The electrical conductivity increased with the increasing MWCNT number density. For the as-prepared film with a MWCNT number density of ~1×10^{10} cm^{-2} (Fig. 3a), they were ~41 and ~6 S cm^{-1} at room temperature, respectively. After the ethanol and pressing treatments with a higher MWCNT number density of ~4×10^{11} cm^{-2} (Fig. 3d), the resulting MWCNT film

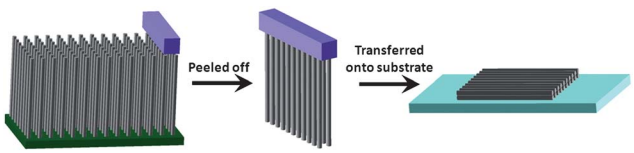

Fig. 2 Schematic illustration of the preparation of the well distributed and aligned CNT film.

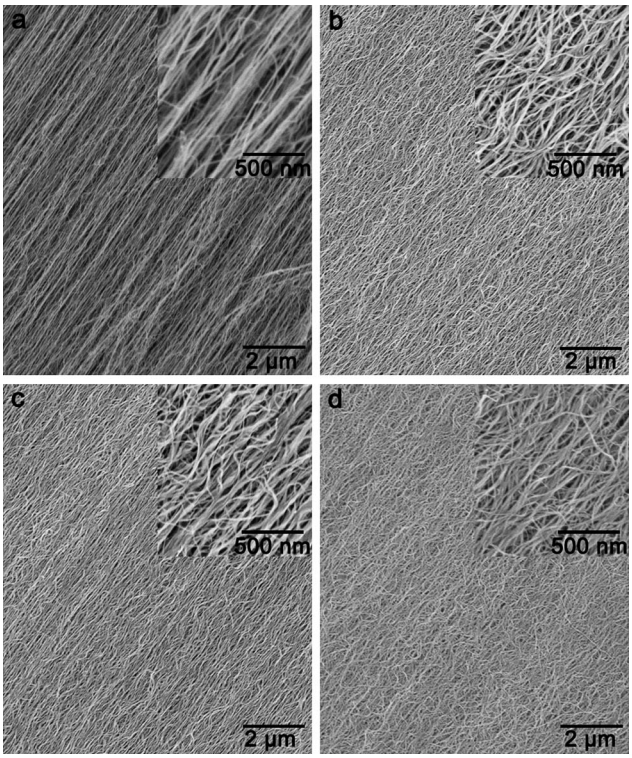

Fig. 3 SEM images of the well distributed and aligned MWCNT films with increasing MWCNT number densities of ~1×10^{10} cm^{-2} (a), ~1×10^{11} cm^{-2} (b), ~3×10^{11} cm^{-2} (c), and ~4×10^{11} cm^{-2} (d) in the cross section (the plane perpendicular to the MWCNT-aligned direction).

showed much improved conductivities of ~1150 and ~223 S cm^{-1}, respectively. Compared with the length direction, the lower conductivities in the width direction were mainly derived from the higher contact resistance among MWCNTs.

To verify the potential application of these MWCNT films as electrodes, particularly flexible electrodes, their electrical resistance in two directions were carefully compared under bending. Fig. 4a and b show that the resistance remained almost unchanged when the MWCNT film on poly (ethylene naphthalate) was bent to 180° with different bending radii in a range from 4 to 14 mm in both directions. Fig. 4c and d further indicate that the resistance varies by less than 1% even after bending for 500 cycles in both directions. The MWCNT film showed much higher resistance stability than a MWCNT sheet which can be prepared only from lower arrays,[13,14,20] and the resulting shorter MWCNTs are more easily destructed under bending.

For use as the counter electrode in a dye-sensitized solar cell it is also necessary to verify the catalytic activity of the MWCNT film. To this end, cyclic voltammetry was performed for the MWCNT film, MWCNT sheet and platinum in an acetonitrile solution containing I_2, LiI, and $LiClO_4$ under the same conditions.[21] Two oxidation/reduction peaks in Fig. 5 clearly indicate the catalytic capability for all three of the electrodes. The left pair of peaks corresponds to the redox reaction in eqn (1) and the right one corresponds to the redox reaction in eqn (2):

$$I_3^- + 2e^- \leftrightarrow 3I^- \quad (1)$$

$$3I_2 + 2e^- \leftrightarrow 3I_3^- \quad (2)$$

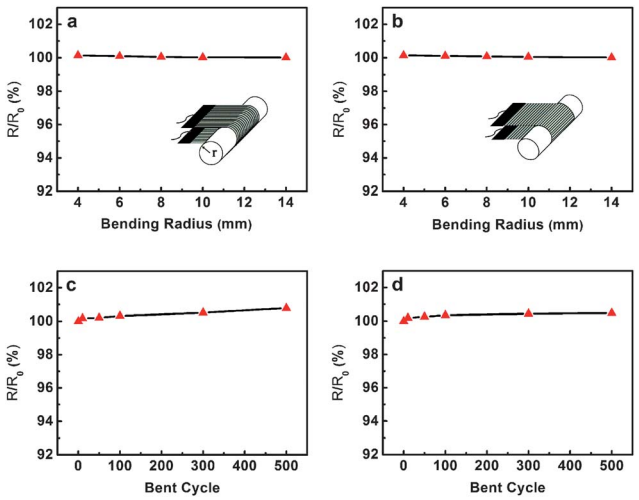

Fig. 4 The electrical resistance of the MWCNT films on poly (ethylene naphthalate) during the bending process. (a) and (c) A film being bent along the length direction. (b) and (d) A film being bent along the width direction. Here R_0 and R correspond to the electrical resistance before and after bending. The inserted images at (a) and (c) schematically show the bending direction. One bent cycle means that a film is bent to 180° (with a bending radius of 4 mm) and then recovered to the original state.

Generally, the catalytic activity of the electrodes is proportional to the reduction peak current density and inversely proportional to the peak-to-peak voltage separation both at the left pair of peaks.[22] Obviously, the reduction peak current density of the MWCNT film is almost two times that of the platinum and 4 times that of the MWCNT sheet. At the same time, the peak-to-peak voltage separation for the MWCNT film is 0.36 V, compared with 0.42 V for the platinum and 0.70 V for the MWCNT sheet. Therefore, the MWCNT film exhibited the best capability for the reduction of I_3^-.

Fig. S4† schematically shows a typical structure of the dye-sensitized solar cell based on the MWCNT film as the counter electrode. Fluorine-doped tin oxide deposited with titanium oxide nanoparticles was used as the working electrode, and *cis*-diisothiocyanato-bis(2,2′-bipyridyl-4,4′-dicarboxylato)

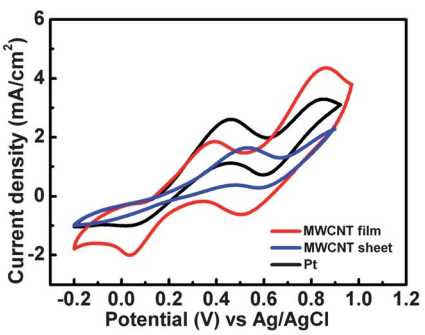

Fig. 5 Comparison of electrocatalytic activities between the MWCNT film (red line), MWCNT sheet (blue line) platinum (black line) electrodes. The cyclic voltammetry was performed in an acetonitrile solution containing 1 mM I_2, 10 mM LiI, and 0.1 M $LiClO_4$ with a scan rate of 100 mV s^{-1} through a three-electrode setup.

ruthenium(II) bis(tetrabutylammonium) (also called N719, and the chemical structure is shown in Fig. S5†) was used as the dye. The resulting dye-sensitized solar cells were expected to show a high performance according to the working mechanism.[23–28] Fig. 6a compares the dye-sensitized solar cells by using the MWCNT film, MWCNT sheet and platinum as counter electrodes measured under AM 1.5 illumination. For a MWCNT film with a thickness of 4 μm and MWCNT number density of $\sim 2 \times 10^{11}$ cm^{-2} derived from an array with a height of 1.5 mm, the resulting cell typically showed an open-circuit voltage (V_{OC}) of 0.74 V, a short-circuit current density (J_{SC}) of 18.02 mA cm^{-2} and a fill factor (FF) of 0.67. Therefore, the energy conversion efficiency (η) was calculated to be 9.00%. As a comparison, if the counter electrode was replaced by the MWCNT sheet while the other parameters such as the material used, the fabrication and the structure were maintained the same, the cell showed V_{OC} of 0.73 V, J_{SC} of 14.84 mA cm^{-2} and FF of 0.58, which produces an η of 6.20%. As another comparison, when the platinum electrode was used under the same conditions the derived cell exhibited a V_{OC} of 0.75 V, J_{SC} of 17.65 mA cm^{-2} and a FF of 0.61, which produces an η of 8.05%. Obviously, in the application as counter electrodes, the MWCNT film shows the best performance. Although it may not be very accurate to directly compare these three kinds of electrodes as their conductivity, thickness, and surface roughness could be different, this comparison did provide a clue that such MWCNT films showed a good potential for the application as counter electrodes in dye-sensitized solar cells.

To better understand the high performance of the MWCNT film, electrochemical impedance spectroscopy was used to compare the cells based on the MWCNT film and platinum as counter electrodes. As shown in Fig. 6b, the serial resistance (R_S) is the combined resistance of electrolyte and electrode, while the resistance of R_{CT1}, R_{CT2}, and R_{diff} (the real part of diffusion impedance, *i.e.*, Z_W) correspond to the electrochemical reaction at the counter electrode in the high-frequency region, the charge transfer at TiO_2/dye/electrode interfaces in the middle-frequency region and the Warburg diffusion process of I^-/I_3^- ions in the electrolyte in the low-frequency region, respectively.[29–31] Therefore, the catalytic capability can be directly reflected by R_{CT1} (the first semicircle at the high frequency). Here the MWCNT film counter electrode exhibited the smallest R_{CT1}. Therefore, it shows a higher catalytic activity than both platinum and the MWCNT sheet. A smaller R_{CT1} reduces the cell resistance to improve both J_{SC} and FF. In other words, the higher cell efficiency based on the MWCNT film should be derived from the higher catalytic activity and higher electrical conductivity, which are further closely related to the uniformly distributed structure of the MWCNTs in the film.

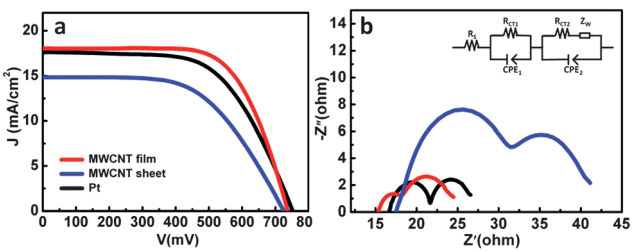

Fig. 6 A comparison of the MWCNT film (red line) with the MWCNT sheet (blue line) platinum (black line) as counter electrodes to fabricate dye-sensitized solar cells. The MWCNT film used with a thickness of 4 μm and MWCNT number density of $\sim 2 \times 10^{11}$ cm^{-2} was prepared from a MWCNT array with a height of 1.5 mm. (a) *J–V* curves of three typical cells measured under AM 1.5 illumination. (b) Nyquist plots of the cells at (a) (the inset image shows an equivalent circuit). The frequencies ranged from 0.1 to 100 kHz with an applied voltage of −0.8 V. Here R_S, R_{CT1}, R_{CT2}, Z_W, and CPE stand for serial resistance, charge-transfer resistance at the counter electrode, charge-transfer resistance at TiO_2/dye/electrode interfaces, diffusion impedance, and constant phase element, respectively.

The aligned MWCNT films with different thicknesses and MWCNT number densities prepared from different heights of used MWCNT arrays were compared for the resulting dye-sensitized solar cells. All the other parameters were kept the same when one was varied. In the case of different thicknesses, both J_{SC} and FF increased with the increasing thickness from 0.5 to 4.0 μm and then slightly decreased with the further increase of film thickness to 10.2 μm, while the V_{OC} remained almost unchanged in the investigated thickness range (Table 1). As a result, the cell efficiency increases with increasing the thickness from 0.5 to 4.0 μm and then slightly decreases with further increase of the film thickness. In other words, a film thickness of 4.0 μm can effectively catalyze the redox reaction of I^-/I_3^- ions. The dependence of the cell parameters on the MWCNT number density has been summarized in Table 2. Both V_{OC} and J_{SC} remained almost unchanged. However, the FF increases with the increasing MWCNT number density up to $\sim 2 \times 10^{11}$ cm^{-2} as the contact resistances reduce with the decreasing distances among the MWCNTs. A further increase in the MWCNT number density to $\sim 4 \times 10^{11}$ cm^{-2} has little effect on decreasing the contact resistances as they remain almost unchanged with the decreasing distances below a critical point. Therefore, the FF was maintained to be almost the same. As a result, the cell efficiency first increases and then remains unchanged with the increasing MWCNT number density. As expected, the cell efficiency slightly increases with increasing the height of the array used (Table 3).

The cell stability based on the MWCNT film was also studied under AM 1.5 at room temperature. Fig. S6† presents the variation in the photovoltaic parameters of MWCNT film based dye-sensitized solar cells with time at room temperature. It was found that both V_{OC} and J_{SC} were increased during the first 72 h and

Table 1 Parameters of the dye-sensitized solar cells using the MWCNT films with the same MWCNT number density of $\sim 2 \times 10^{11}$ cm^{-2} but different thicknesses as counter electrodes measured under AM 1.5 illumination. The MWCNT films were prepared from the same array with height of 1.5 mm

Film thickness	V_{OC} (mV)	J_{SC} (mA cm^{-2})	FF	η (%)
0.5 μm	728	16.10	0.56	6.55
1.0 μm	720	17.05	0.62	7.64
2.1 μm	731	18.18	0.66	8.83
4.0 μm	737	18.02	0.67	8.96
6.2 μm	741	18.23	0.67	8.85
8.6 μm	734	17.57	0.68	8.71
10.2 μm	724	18.11	0.66	8.63

Table 2 Parameters of dye-sensitized solar cells using the MWCNT films with the same thickness of ~2 μm but different MWCNT number densities as counter electrodes measured under AM 1.5 illumination. The MWCNT films were prepared from the same array with height of 1.5 mm

MWCNT number density	V_{OC} (mV)	J_{SC} (mA cm^{-2})	FF	η (%)
~1×10^{10} cm^{-2}	736	17.69	0.58	7.49
~1×10^{11} cm^{-2}	740	17.67	0.63	8.26
~2×10^{11} cm^{-2}	737	17.98	0.68	8.95
~3×10^{11} cm^{-2}	742	17.78	0.68	8.98
~4×10^{11} cm^{-2}	738	18.11	0.67	8.91

Table 3 Parameters of dye-sensitized solar cells using the MWCNT films which were prepared from arrays with different heights as the counter electrodes measured under AM 1.5 illumination. The thickness and number density of the films were the same as ~2 μm and ~2×10^{11} cm^{-2}, respectively

Height of MWCNT array	V_{OC} (mV)	J_{SC} (mA cm^{-2})	FF	η (%)
1 mm	735	17.84	0.68	8.86
2 mm	741	18.18	0.66	8.91
3 mm	737	18.02	0.67	8.95
4 mm	740	18.23	0.67	9.05

then remained almost unchanged, while the FF was stable in the tested duration. Similar phenomena has been observed in many other solar cells.[27,32] A possible explanation is related to the fact that it took time for the electrolyte to infiltrate into the nanomaterial in the electrode and both V_{OC} and J_{SC} were improved during the infiltration process. For the cell based on the MWCNT film, the infiltration was completed in ~72 h. As a result, the cell efficiency was increased in the first 72 h and then stabilized at ~9.05%.

The MWCNT film could also be used as a counter electrode to fabricate flexible dye-sensitized solar cells. At this point, the resulting cells using the MWCNT sheet and film have been compared in Fig. 7. In the case of the MWCNT sheet, V_{OC}, J_{SC}, and FF were 0.68 V, 4.84 mA cm^{-2}, and 0.37, respectively. η was then calculated to be 1.22%. As a comparison, the cell based on the MWCNT film as the counter electrode shows V_{OC}, J_{SC} and FF of 0.76 V, 5.44 mA cm^{-2} and 0.56, respectively, which produces an η of 2.32%. Obviously, all three parameters of V_{OC}, J_{SC} and FF were improved. In particular, FF was improved by ~51% and η was increased by 90%. The difference can be explained by the fact that, due to the more uniform distribution, the MWCNTs in the film more effectively contact the substrate compared with the MWCNT sheet. It should be noted that the shape of the *J–V* curve for the MWCNT sheet was also different from the MWCNT film due to a lot of series resistance between the MWCNT sheet and substrate. As previously reported, MWCNT sheets could not closely and tightly contact with the substrate.[13]

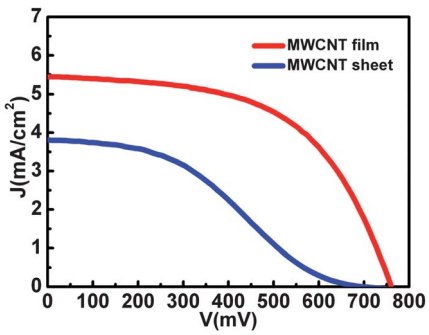

Fig. 7 Typical *J–V* curves of a flexible dye-sensitized solar cell using the MWCNT film (red line) and the MWCNT sheet (blue line) as the counter electrode measured under AM 1.5 illumination. The used MWCNT film with a thickness of 4 μm and MWCNT number density of 2×10^{11} cm^{-2} was prepared from an array with height of 1.5 mm.

Conclusions

In summary, a general approach had been developed to prepare well distributed and aligned MWCNT films with high electrical conductivity and high electrocatalytic activity. When they were used as new counter electrodes to fabricate dye-sensitized solar cells a high efficiency of 9.05% was achieved.

Acknowledgements

This work was supported by NSFC (20904006, 91027025), MOST (2011CB932503, 2011DFA51330), MOE (NCET-09-0318), and STCSM (1052nm01600, 11520701400).

Notes and references

1 B. Kippelen and J. L. Bredas, *Energy Environ. Sci.*, 2009, **2**, 251.
2 M. D. Kelzenberg, S. W. Boettcher, J. A. Petykiewicz, D. B. Turner-Evans, M. C. Putnam, E. L. Warren, J. M. Spurgeon, R. M. Briggs, N. S. Lewis and H. A. Atwater, *Nat. Mater.*, 2010, **9**, 239.
3 R. F. Service, *Science*, 2011, **332**, 293.
4 A. Yella, H.-W. Lee, H. N. Tsao, C. Yi, A. K. Chandiran, M. K. Nazeeruddin, E. W.-G. Diau, C.-Y. Yeh, S. M. Zakeeruddin and M. Graetzel, *Science*, 2011, **334**, 629.
5 A. Hagfeldt, G. Boschloo, L. C. Sun, L. Kloo and H. Pettersson, *Chem. Rev.*, 2010, **110**, 6595.
6 B. Oregan and M. Gratzel, *Nature*, 1991, **353**, 737.
7 S. I. Cha, B. K. Koo, S. H. Seo and D. Y. Lee, *J. Mater. Chem.*, 2010, **20**, 659.
8 M. I. Asghar, K. Miettunen, J. Halme, P. Vahermaa, M. Toivola, K. Aitola and P. Lund, *Energy Environ. Sci.*, 2010, **3**, 418.
9 G. R. Li, F. Wang, Q. W. Jiang, X. P. Gao and P. W. Shen, *Angew. Chem., Int. Ed.*, 2010, **49**, 3653.
10 Y. C. Lan, Y. Wang and Z. F. Ren, *Adv. Phys.*, 2011, **60**, 553.
11 J. Han, H. Kim, D. Y. Kim, S. M. Jo and S. Y. Jang, *ACS Nano*, 2010, **4**, 3503.
12 X. Mei, S. J. Cho, B. Fan and J. Ouyang, *Nanotechnology*, 2010, **21**, 395202.
13 H. Peng, *J. Am. Chem. Soc.*, 2008, **130**, 42.
14 Z. Yang, T. Chen, R. He, G. Guan, H. Li and H. Peng, *Adv. Mater.*, 2011, **23**, 5636.
15 H. Peng and X. Sun, *Chem. Commun.*, 2009, 1058.
16 W. Guo, C. Liu, X. Sun, Z. Yang, H. G. Kia and H. Peng, *J. Mater. Chem.*, 2012, **22**, 903.
17 Z. Yang, X. Sun, X. Chen, Z. Yang, G. Xu, R. He, Z. An, Q. Li and H. Peng, *J. Mater. Chem.*, 2011, **21**, 13772.
18 H. Peng, J. Menka, D. E. Peterson, Y. Zhu and Q. Jia, *Small*, 2008, **4**, 1964.
19 N. Papageorgiou, W. E. Maier and M. Grätzel, *J. Electrochem. Soc.*, 1997, **144**, 876.
20 K. Liu, Y. Sun, P. Liu, X. Lin, S. Fan and K. Jiang, *Adv. Funct. Mater.*, 2011, **21**, 2721.
21 C. H. Yoon, R. Vittal, J. Lee, W. S. Chae and K. J. Kim, *Electrochim. Acta*, 2008, **53**, 2890.

22 X. Lin, M. Wu, Y. Wang, A. Hagfeldt and T. Ma, *Chem. Commun.*, 2011, **47**, 11489.
23 J. Wang and M. Musameh, *Anal. Chem.*, 2003, **75**, 2075.
24 H. Zhu, H. Zeng, V. Subramanian, C. Masarapu, K. Huang and B. Wei, *Nanotechnology*, 2008, **19**, 465204.
25 J. G. Nam, Y. J. Park, B. S. Kim and J. S. Lee, *Scr. Mater.*, 2010, **62**, 148.
26 J. Liu, Y. Kuo, K. J. Klabunde, C. Rochford, J. Wu and J. Li, *ACS Appl. Mater. Interfaces*, 2009, **1**, 1645.
27 J. E. Trancik, S. C. Barton and J. Jone, *Nano Lett.*, 2008, **8**, 982.
28 W. J. Lee, E. Ramasamy, D. Y. Lee and J. S. Song, *ACS Appl. Mater. Interfaces*, 2009, **1**, 1145.
29 E. Ramasamy, W. J. Lee, D. Y. Lee and J. S. Song, *Electrochem. Commun.*, 2008, **10**, 1087.
30 A. Kay and M. Grätzel, *Sol. Energy Mater. Sol. Cells*, 1996, **44**, 99.
31 E. Ramasamy, W. J. Lee, D. Y. Lee and J. S. Song, *Appl. Phys. Lett.*, 2007, **90**, 173103.
32 H. Choi, C. Baik, S. O. Kang, J. Ko, M. Kang, M. K. Nazeeruddin and M. Gratzel, *Angew. Chem., Int. Ed.*, 2008, **47**, 327.

